

IMMUNOTHERAPY

Gasdermin E-mediated target cell pyroptosis by CAR T cells triggers cytokine release syndrome

Yuying Liu^{1,2*}, Yiliang Fang^{1*}, Xinfeng Chen^{3*}, Zhenfeng Wang¹, Xiaoyu Liang¹, Tianzhen Zhang¹, Mengyu Liu¹, Nannan Zhou¹, Jiadi Lv¹, Ke Tang⁴, Jing Xie¹, Yunfeng Gao¹, Feiran Cheng¹, Yabo Zhou¹, Zhen Zhang³, Yu Hu⁵, Xiaohui Zhang⁶, Quanli Gao⁷, Yi Zhang³, Bo Huang^{1,2,4†}

Copyright © 2020
The Authors, some
rights reserved;
exclusive licensee
American Association
for the Advancement
of Science. No claim
to original U.S.
Government Works

Cytokine release syndrome (CRS) counteracts the effectiveness of chimeric antigen receptor (CAR) T cell therapy in cancer patients, but the mechanism underlying CRS remains unclear. Here, we show that tumor cell pyroptosis triggers CRS during CAR T cell therapy. We find that CAR T cells rapidly activate caspase 3 in target cells through release of granzyme B. The latter cleaves gasdermin E (GSDME), a pore-forming protein highly expressed in B leukemic and other target cells, which results in extensive pyroptosis. Consequently, pyroptosis-released factors activate caspase 1 for GSDMD cleavage in macrophages, which results in the release of cytokines and subsequent CRS. Knocking out GSDME, depleting macrophages, or inhibiting caspase 1 eliminates CRS occurrence in mouse models. In patients, GSDME and lactate dehydrogenase levels are correlated with the severity of CRS. Notably, we find that the quantity of perforin/granzyme B used by CAR T cells rather than existing CD8⁺ T cells is critical for CAR T cells to induce target cell pyroptosis.

INTRODUCTION

Despite the success of clinical applications of genetically engineered T cells modified with chimeric antigen receptors (CARs) against B cell malignancies (1–3), cytokine release syndrome (CRS) hinders the effectiveness of this treatment in patients (4, 5). It is known that CRS is triggered by acute inflammatory responses and characterized by fever, hypotension, and respiratory insufficiency associated with elevated serum cytokines (5–7). Although macrophages have been reported to be involved in the pathogenesis of CRS in the CAR T cell-treated humanized mouse model (8, 9), the mechanisms triggering CRS are unclear. CAR T cells undergo activation and expansion in patients after their infusion (5, 10, 11), and rapidly expanded CAR T cells may result in a rapid and massive death of B leukemic cells within a brief period. Coincidentally, disease burden in patients with acute lymphoblastic leukemia is also strongly correlated with the incidence and severity of CRS (5, 10–12). The manner by which such a massive malignant B cell death is involved in CRS pathogenesis remains elusive.

Cells can undergo distinct types of death. Apoptosis was originally considered the only form of controlled and programmed death. However, recent studies have demonstrated a previously unidentified form of programmed necrosis, characterized by rapid cellular swelling, large bubbles emerging from the plasma membrane, and the release of pro-

inflammatory factors (13, 14). At least two programmed necrotic cell death pathways have been identified, including a mixed lineage kinase domain-like (MLKL)-mediated necroptosis (15, 16) and gasdermin D (GSDMD)- or GSDME-mediated pyroptosis (17, 18). Recruitment of receptor-interacting protein kinase 1 (RIPK1) to the tumor necrosis factor- α (TNF- α) receptor forms a death complex with RIP3 and subsequently activates MLKL to generate membrane nan pores, thus causing necrotic cell death (19). Unlike MLKL, GSDMD or GSDME is activated by inflammatory caspases (caspases 1, 4, and 5 and murine caspase 11) or caspase 3 (17, 20) and can form oligomers that insert into the cell membranes to form pores, thus mediating pyroptotic cell death. In this study, we provide evidence that human B leukemic cells and other target tumor cells express a sufficient amount of GSDME, which is efficiently activated by CAR T cell-released granzyme B-activated caspase 3, leading to target cell pyroptosis. Pyroptosis-released factors stimulate macrophages to produce proinflammatory cytokines, which is likely triggering CRS in CAR T cell-treated patients.

RESULTS

CAR T cells induce target cell pyroptosis

When we incubated CD19-recognizing CAR T cells with CD19⁺ primary leukemic cells isolated from B cell acute lymphoblastic leukemia (B-ALL) patients, we found that the viability of B leukemic cells markedly decreased, whereas human epidermal growth factor receptor 2 (HER2)-specific CAR T cells did not have such an effect (Fig. 1A). We observed that the dying cells appeared to have a swollen appearance with large bubbles arising from the plasma membrane (Fig. 1B). Flow cytometric analysis showed that more than 30% of CAR T cell-treated CD19⁺ B leukemic cells were annexin V⁺ and propidium iodide (PI)⁺ (Fig. 1C). High levels of lactate dehydrogenase (LDH) were present in the supernatants (Fig. 1D), suggesting that CAR T cells induce pyroptosis in CD19⁺ B leukemic cells. We also found that CD19-CAR T cells induced pyroptosis in CD19⁺ Raji and NALM-6 leukemic cell lines in a time- and effector/target ratio-dependent manner, as indicated by decreased cell viability, cellular swelling with bubbles,

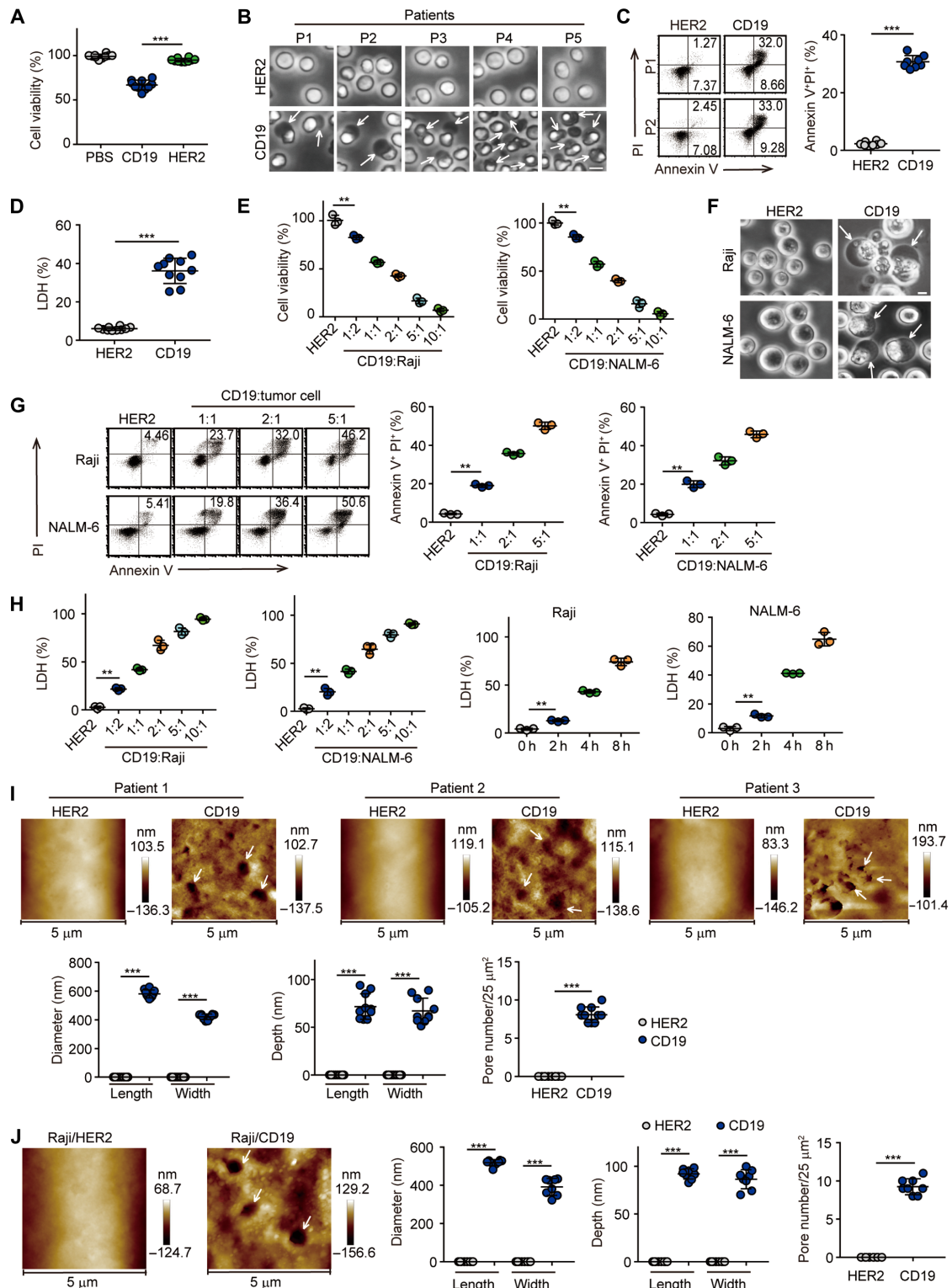
¹Department of Immunology and National Key Laboratory of Medical Molecular Biology, Institute of Basic Medical Sciences, Chinese Academy of Medical Sciences (CAMS) and Peking Union Medical College, Beijing 100005, China. ²Clinical Immunology Center, CAMS, Beijing 100005, China. ³Biotherapy Center and Cancer Center, First Affiliated Hospital of Zhengzhou University, Zhengzhou 450052, Henan, China.

⁴Department of Biochemistry and Molecular Biology, Tongji Medical College, Huazhong University of Science and Technology, Wuhan 430030, China. ⁵Institute of Hematology, Union Hospital, Tongji Medical College, Huazhong University of Science and Technology, Wuhan 430022, China. ⁶Peking University People's Hospital, Peking University Institute of Hematology, Beijing 100044, China. ⁷Department of Immunology, Affiliated Cancer Hospital of Zhengzhou University and Henan Cancer Hospital, Zhengzhou, Henan 450008, China.

*These authors contributed equally to this work.

†Corresponding author. Email: tjhuangbo@hotmail.com

Fig. 1. CAR T cells induced tumor cell pyroptosis. (A to D) Primary B leukemic cells were cocultured with CD19 or HER2-CAR T cells at an effector/target ratio (E/T) of 2:1 for 6 hours. Tumor cell viability was measured by using the CellTiter-Glo Luminescent Cell Viability Assay Kit [(A), $n = 10$]. The representative images were shown (B). Cell death was determined by flow cytometry [(C), $n = 6$], and LDH level in the supernatants was measured [(D), $n = 10$]. Scale bar, 20 μ m. White arrows indicate pyroptotic cells. (E to H) Luc-Raji or NALM-6 cells were cocultured with CD19- or HER2-CAR T cells at different ratios as indicated for 4 hours or at the ratio of 1:1 for the indicated time. Cell viability was measured (E), and the representative images were shown (F). The percentage of annexin V⁺/PI⁺ tumor cells was determined by flow cytometry (G). LDH levels in the supernatants were measured (H). Scale bar, 10 μ m. (I) The same as (A), except that primary B leukemic cells were imaged by AFM. Pore diameter and depth were calculated within a cellular membrane area of 5 μ m by 5 μ m from 10 cells. Pore number was quantified from three areas of 5 μ m by 5 μ m per cell. A pore was defined as a cavity deeper than 10 nm in the plasma membrane. White arrows indicate pores. (J) Raji cells were cocultured with CD19-CAR T cells for 1 hour. Pore size and number were measured and counted. ** $P < 0.01$, *** $P < 0.001$, by Student's *t* test (C, D, I, and J) or one-way ANOVA (A, E, G, and H). Data are means \pm SD of three independent experiments.



an increased percentage of annexin V⁺/PI⁺ cells, and high levels of LDH (Fig. 1, E to H, and fig. S1A). Pyroptosis is known to be mediated by gasdermins such as GSDMD and GSDME, which form pores in the plasma membrane (17, 20, 21). Recently, we developed an atomic force microscopy (AFM)-based technology to visualize pore forma-

tion in true cellular membranes (22). Using this method, we observed that many pores were formed in the membrane of the B leukemic cells after coculture with CD19-CAR T cells (Fig. 1, I and J, and fig. S1B), further supporting the idea that B leukemic cells underwent pyroptosis. Other CAR T cells such as HER2-recognition CAR, incubated with

HER2⁺ solid tumor cells (MCF-7 and SGC-7901), also caused decreased cell viability, swelling with bubbles, LDH release, and pore formation in tumor cells (fig. S1, C to F, and movies S1 and S2). Together, these results suggest that CAR T cell therapy may induce target tumor cells to enter pyroptosis.

CAR T cells activate GSDME to mediate target cell pyroptosis

It is known that activated inflammatory caspases (caspases 1, 4, 5, and 11) or caspase 3 can cleave GSDMD or GSDME to generate its active form, which inserts into the cellular membranes causing pore formation and subsequent cellular pyroptosis (17, 21). GSDME, but

not GSDMD, was ubiquitously expressed in the CD19⁺ malignant B cells of patients (Fig. 2A). In addition, CD19⁺ Raji and NALM-6 cells and HER2⁺ SGC-7901 and MCF-7 tumor cells also expressed high levels of GSDME (Fig. 2A), and the active form of GSDME was induced by CAR T cells in CD19⁺ or HER2⁺ tumor cells (Fig. 2B and fig. S2A). MLKL is also able to form pores in the cell membrane and induce necroptosis (16), but the phosphorylated form of MLKL and RIPK1/3 was not detectable in tumor cells (fig. S2A). These results suggest that GSDME rather than other molecules mediates CAR T cell-triggered tumor cell pyroptosis. To verify this, we knocked out GSDME in four types of target cells (Raji, NALM-6, SGC-7901,

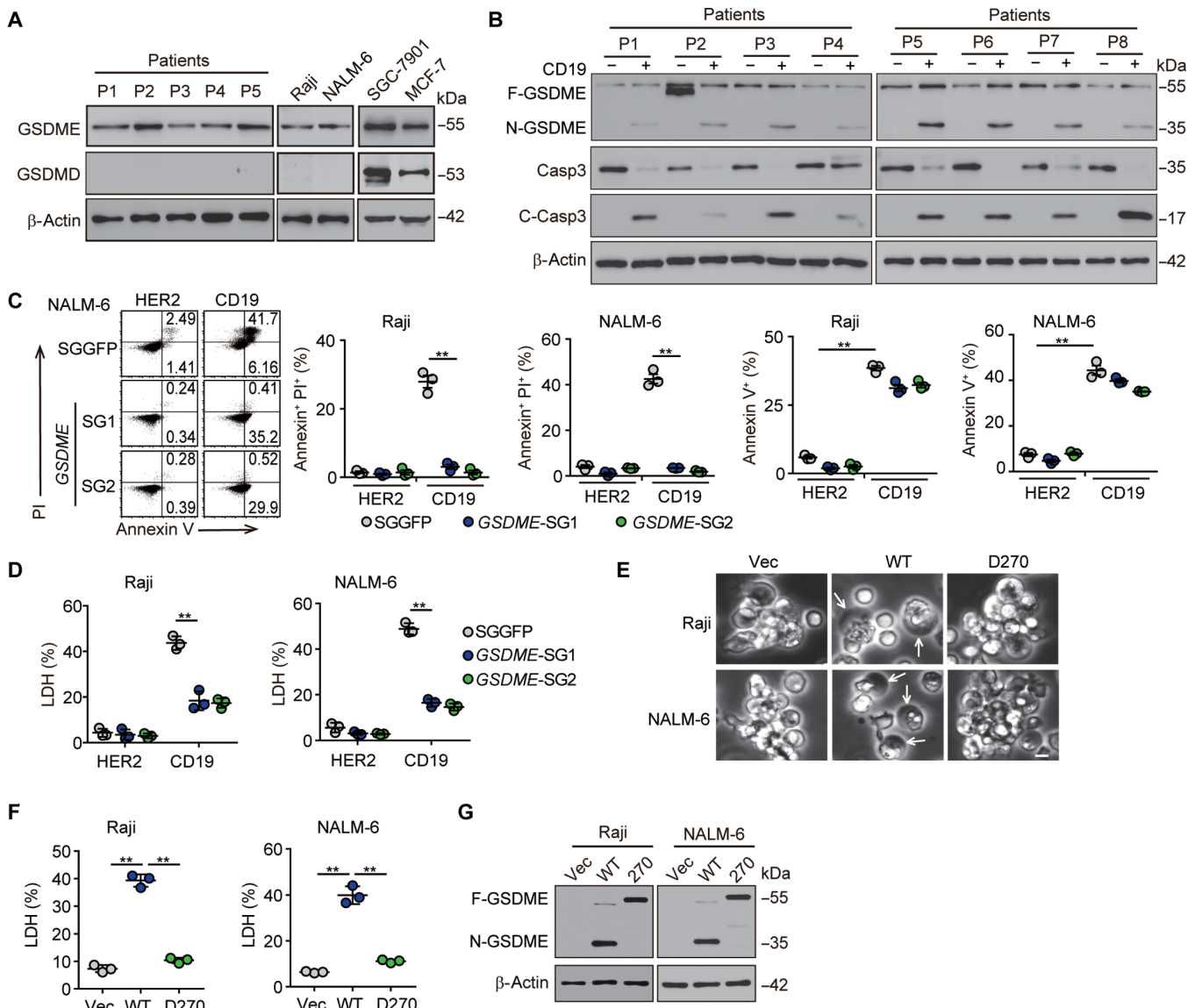


Fig. 2. Tumor cell pyroptosis by CAR T cells is mediated by GSDME. (A) GSDME and GSDMD in primary B leukemic cells isolated from B-ALL patients ($n = 5$) or cell lines were determined by Western blot. (B) CD19⁺ B leukemic cells from B-ALL patients ($n = 8$) were cocultured with or without CD19-CAR T cells for 6 hours. GSDME, caspase 3 (Casp3), and cleaved caspase 3 (C-Casp3) were analyzed by Western blot. (C and D) SGGFP or GSDME-SGs⁻ Raji or NALM-6 cells were cocultured with HER2 or CD19-CAR T cells for 4 hours. The percentage of annexin V⁺/PI⁺ or annexin V⁺ cells (C) and the LDH level from the supernatant (D) were measured. (E to G) GSDME-deficient Raji or NALM-6 cells with overexpressed vector, WT-GSDME, or D270-GSDME were cocultured with CD19-CAR T cells at an E/T ratio of 2:1 for 4 hours. Cell morphology was observed under a microscope (E). The LDH level from the supernatant was detected (F). The expression of GSDME was determined by Western blot (G). Scale bar, 20 μ m. White arrows indicate the pyroptotic cell. ** $P < 0.01$, by one-way ANOVA (C, D, and F). Data are means \pm SD of three independent experiments.

and MCF-7) and found that GSDME deficiency, which did not affect tumor cell growth (fig. S2, B and C), abrogated CAR T cell–induced target cell pyroptosis, as indicated by the decreased percentage of annexin V⁺/PI⁺ cells and reduced levels of LDH in supernatants (Fig. 2, C and D, and fig. S2, D and E). However, overexpression of GSDME increased pyroptosis of target cells (fig. S2, F and G), suggesting that CAR T cells trigger tumor cell pyroptosis by activating GSDME. Despite the pyroptosis mediated by GSDME, the blockade of GSDME actually resulted in target cell death switching from pyroptosis to apoptosis (Fig. 2C and fig. S2D). In line with this observation, normal B cells did not express GSDME (fig. S2H) and could also be triggered to undergo apoptosis by CD19-CAR T cells (fig. S2, I and J). To validate this idea, we introduced GSDME-expressing vectors to the GSDME-deficient tumor cells and found that the re-expression of GSDME restored CAR T cell–induced pyroptosis (Fig. 2, E and F). However, the reexpression of mutant GSDME (D270A) could not restore the pyroptosis from the apoptosis (Fig. 2, E and F). Consistent with this observation, the active form of GSDME was not found in GSDME (D270A)–expressing cells (Fig. 2G). Together,

these results suggest that CAR T cells can mobilize GSDME to induce target cell pyroptosis.

CAR T cell-released granzyme B triggers the cleavage of GSDME

To better understand the molecular mechanism that CAR T cells use to activate GSDME in tumor cells, we measured caspase 3 cleavage by Western blot (17). As expected, caspase 3, but not caspase 1 or caspase 4, was cleaved and activated in co-incubated tumor cells (Figs. 2B and 3A and fig. S3A). Moreover, the addition of the caspase 3 inhibitor DEVD or the pan-caspase inhibitor zVAD inhibited the cleavage of GSDME and prevented tumor cell pyroptosis (fig. S3, B to D). In contrast, we found that GSDME knockout did not affect caspase 3 activation, suggesting that GSDME functions downstream of caspase 3 (fig. S3E). Granzyme B, which is released from cytolytic T cells, is a key effector molecule that cleaves caspases 3 and 7 to generate their active forms (23, 24). We found that inhibition of granzyme B in CAR T cells by small interfering RNA (siRNA) or a chemical compound (GrBI) blocked the activation of caspases 3 and

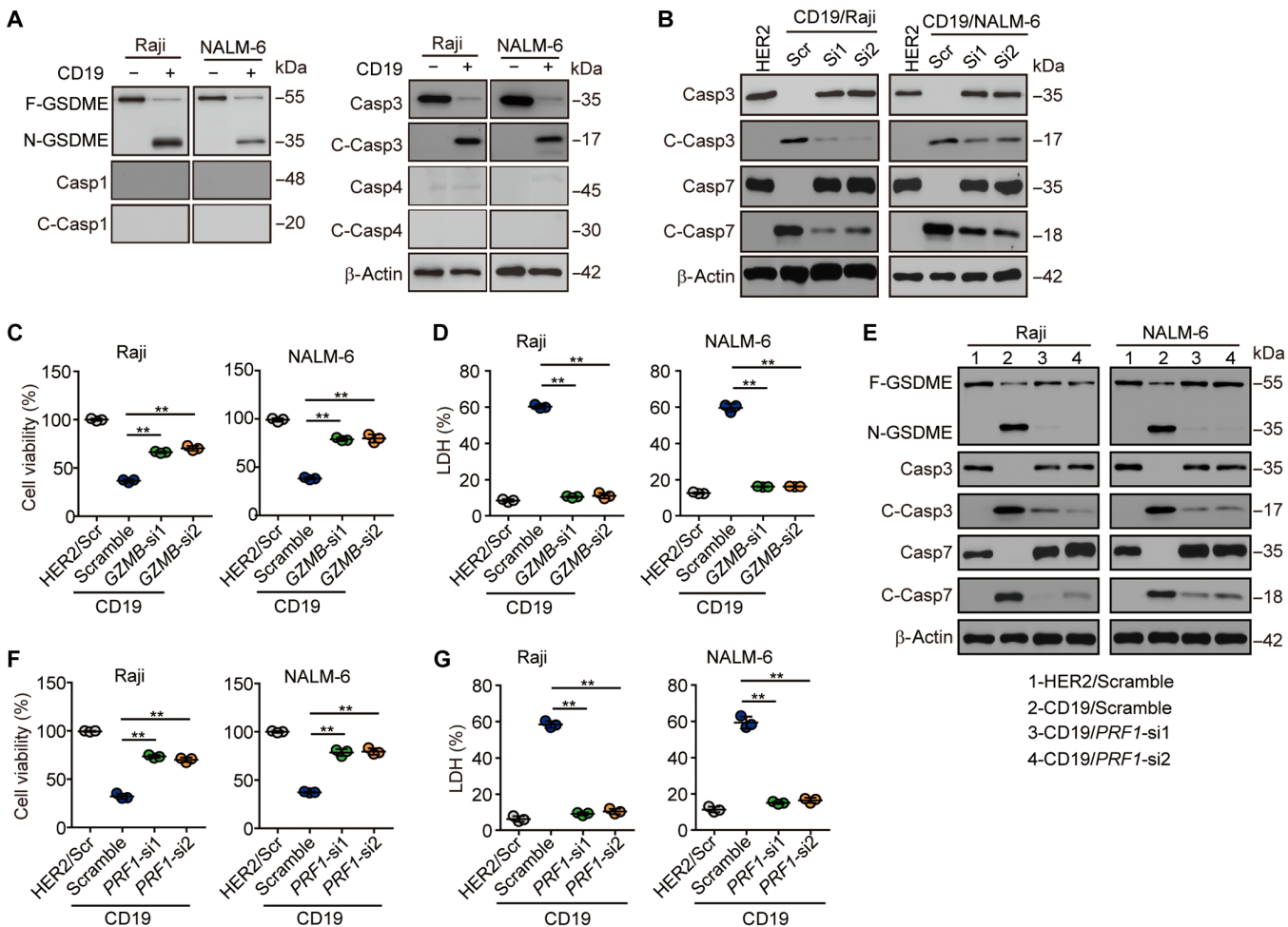


Fig. 3. CAR T cell-released granzyme B triggers the activation of GSDME. (A) CD19⁺ Raji or NALM-6 cells were cocultured with or without CD19-CAR T cells for 4 hours. GSDME, Casp1, C-Casp1, Casp3, C-Casp3, Casp4, and C-Casp4 were analyzed by Western blot. (B to D) Scramble (Scr) or GZMB-siRNAs[−] CD19-CAR T cells were cocultured with Luc-Raji or NALM-6 cells for 4 hours. Casp3, C-Casp3, Casp7, and C-Casp7 were analyzed by Western blot (B). Cell viability (C) and LDH levels in the supernatants (D) were measured. (E to G) The same as (B) to (D), except that PRF1-siRNAs[−] CD19-CAR T cells were used. **P < 0.01, by one-way ANOVA (C, D, F, and G). Data are means ± SD of three independent experiments.

7 in tumor cells, thus inhibiting pyroptosis (Fig. 3, B to D, and fig. S3, F to I). Perforin pore formation allows granzyme B to enter the cytosol of target cells (25), and perforin knockdown prevented the activation of caspases 3 and 7, cleavage of GSDME, and subsequent pyroptosis (Fig. 3, E to G, and fig. S3F). These results suggest that CAR T cells release perforin to form pores, leading to the entry of granzyme B into target tumor cells, which causes the subsequent activation of GSDME and pyroptosis.

Superior affinity to target cells is critical for CAR T cells to trigger pyroptosis

The above data indicated that CAR T cells used perforin/granzyme B to induce tumor cell pyroptosis. However, nontransduced CD8⁺ T cells can use the same perforin and granzyme B mechanism to attack target cells, leading to tumor cell apoptosis rather than pyroptosis (26). To better define this mechanism, we constructed human CD19-recognizing mouse CAR (hCD19-mCAR) in murine OT-I T cells and human CD19- or human HER2-expressing B16 melanoma cells. Incubation of OT-I hCD19-mCAR T cells with CD19-B16 cells triggered pyroptosis, but this was not observed in HER2-B16 cells or vector-B16 cells, and ovalbumin (OVA) peptide-pulsed B16 cells underwent apoptosis (Fig. 4, A to C). In addition, we found that, even when the incubation time was prolonged, the pulsed B16 cells did not display cellular swelling or membrane bubbles (fig. S4A), suggesting that nontransduced tumor-specific T cells do not induce target tumor cell pyroptosis. Consistently, unmodified OT-I T cells released perforin/granzyme B to induce OVA-B16 apoptosis rather than pyroptosis (fig. S4, B and C). Similarly, allogeneic CD8⁺ T cells isolated from donors also used perforin/granzyme B to induce apoptosis in MCF-7 or SGC-7901 cells rather than pyroptosis (fig. S4, D and E). Knockdown of either perforin or granzyme B inhibited the killing of OVA-B16 or B16 tumor cells by OT-I or pmel T cells (fig. S4F), raising a question as to why CAR T cell–but not tumor-specific T cell–derived perforin/granzyme B induced pyroptosis. One explanation is that the quantity of perforin/granzyme B released from CAR T cells and from unmodified CD8⁺ T cells may be different. It is known that the affinity of CAR and its antigen may be 100-fold higher than that of T cell receptor (TCR) and major histocompatibility complex (MHC)–peptide complex (27, 28). We speculated that the CAR-antigen interaction resulted in more perforin/granzymes being released by CAR T cells. OT-I hCD19-mCAR T cells released more perforin/granzyme B after coculture with hCD19-B16 cells, as compared with HER2-B16 or OVA peptide-pulsed B16 cells (Fig. 4D). Although allogeneic CD8⁺ T cells could kill MCF-7 or SGC-7901 tumor cells in the presence of a CD28 antibody (fig. S4D), these CD8⁺ T cells expressed much lower levels of CD107a than the corresponding CAR T cells (fig. S4G), and less granzyme B was present in the target tumor cells during incubation with allogeneic T cells (fig. S4H). Moreover, we found that tumor-specific T cells induced a small amount of GSDME cleavage and did not activate GSDMD or MLKL, regardless of the cleavage of caspases 3 and 7 in tumor cells (fig. S4I). Cells have the ability to rapidly repair the formed membrane pore (22, 29), thus preventing cell pyroptosis induced by a small amount of GSDME activated by caspase 3. Therefore, only a large amount of active GSDME can surpass the pore-repairing ability of the cell and lead to pyroptosis. As expected, high levels of cleaved GSDME was present in CD19-B16 cells after incubation with CD19-CAR T cells (Fig. 4E), and a GSDME knockout abolished the effect of CAR T cells on CD19-B16 cell pyroptosis (Fig. 4, F and G). However,

the knockout of GSDME had less influence on B16 cell apoptosis induced by OT-I T cells (Fig. 4, F and H). The addition of exogenous perforin/granzyme B to the medium led to OVA-B16 or B16 cell pyroptosis by tumor-specific T cells (Fig. 4, I to K). In addition, the use of recombinant perforin and granzyme B to treat tumor cells induced tumor cell death by either apoptosis or pyroptosis dependent on the dosage (low or high) (fig. S5, A to C). In addition to the superior affinity of CAR to tumor cell antigen, we also investigated whether the co-signaling domains in CD19-CAR played a role in regulating target cell pyroptosis. We constructed CD19-CAR with CD3ζ domains, but without CD28 signaling domains, and cocultured with CD19-expressing B16 cells in the presence of a CD28 antibody. We found that compared with CD3ζ-CD28-CAR T cells, CD3ζ-CAR T cells had much less of an effect on the decreased cell viability, increased LDH levels, and the induction of annexin V⁺/PI⁺ cells (Fig. 5, A to C). CD3ζ-CAR T cells appeared to not induce tumor cell pyroptosis, as evidenced by the lack of cellular swelling and membrane bubbles (Fig. 5D). In addition, we found that CD19-CAR T cells with different co-signaling domains (CD3ζ-CD28, CD3ζ-4-1BB, or CD3ζ-CD28-4-1BB) could induce CD19-B16 cells to enter pyroptosis (Fig. 5, E to G). Among them, CD3ζ-CD28-4-1BB-CD19-CAR T cells exerted the strongest effect on pyroptosis, whereas CD3ζ-CD28 and CD3ζ-4-1BB-CD19-CAR T cells had a similar effect (Fig. 5, E to G). Together, these results suggest that superior tumor antigen affinity and the co-signaling domains confer CAR T cells with the ability to release large amounts of perforin/granzyme B required for CAR T cell-mediated tumor cell pyroptosis.

Target cell pyroptosis stimulates macrophages to release CRS-related cytokines

Pyroptotic cells release large amounts of damage-associated molecular pattern molecules (DAMPs), which can trigger strong inflammatory responses like CRS, prompting us to hypothesize that GSDME-mediated pyroptosis triggers CRS during CAR T cell therapy. Macrophages are involved in inflammatory responses and have been reported to play an important role in CAR T cell therapy-induced CRS (8, 9). When cocultured supernatants (CD19-CAR T cells and NALM-6, Raji, or primary B leukemic cells) were used to treat macrophages derived from the peripheral blood mononuclear cells (PBMCs) of healthy donors, we observed a marked release of interleukin-1β (IL-1β) and IL-6, two markers of CRS (Fig. 6, A and B, and fig. S6A). Supernatants from HER2-CAR T/SGC-7901 cells also resulted in the release of these two cytokines by treated macrophages (fig. S6B), indicating that CRS can be triggered by products of tumor cell pyroptosis. However, supernatants from nontransduced tumor-specific CD8⁺ T cells that killed target tumor cells did not stimulate macrophages to secrete IL-1β or to up-regulate the expression of IL-6 (fig. S6C). To validate these results, we used CD19 or HER2-CAR T cells to coculture with GSDME^{-/-} target cells (NALM-6, Raji, or SGC-7901). Under this condition, the supernatants were not able to stimulate macrophages to produce IL-1β or IL-6 (Fig. 6C and fig. S6D). It is known that macrophages release IL-1β through the activation of the inflammasome pathway. Caspase 1, the effector molecule of inflammasomes that cleaves pro-IL-1β, was activated in macrophages by the above pyroptotic supernatants, whereas supernatants from the GSDME knockout groups did not cause the cleavage of caspase 1 in macrophages (Fig. 6D). In addition to IL-1β, caspase 1 also cleaves and generates the active form of GSDMD, the membrane pore-forming molecule, which leads to the release of IL-1β and other

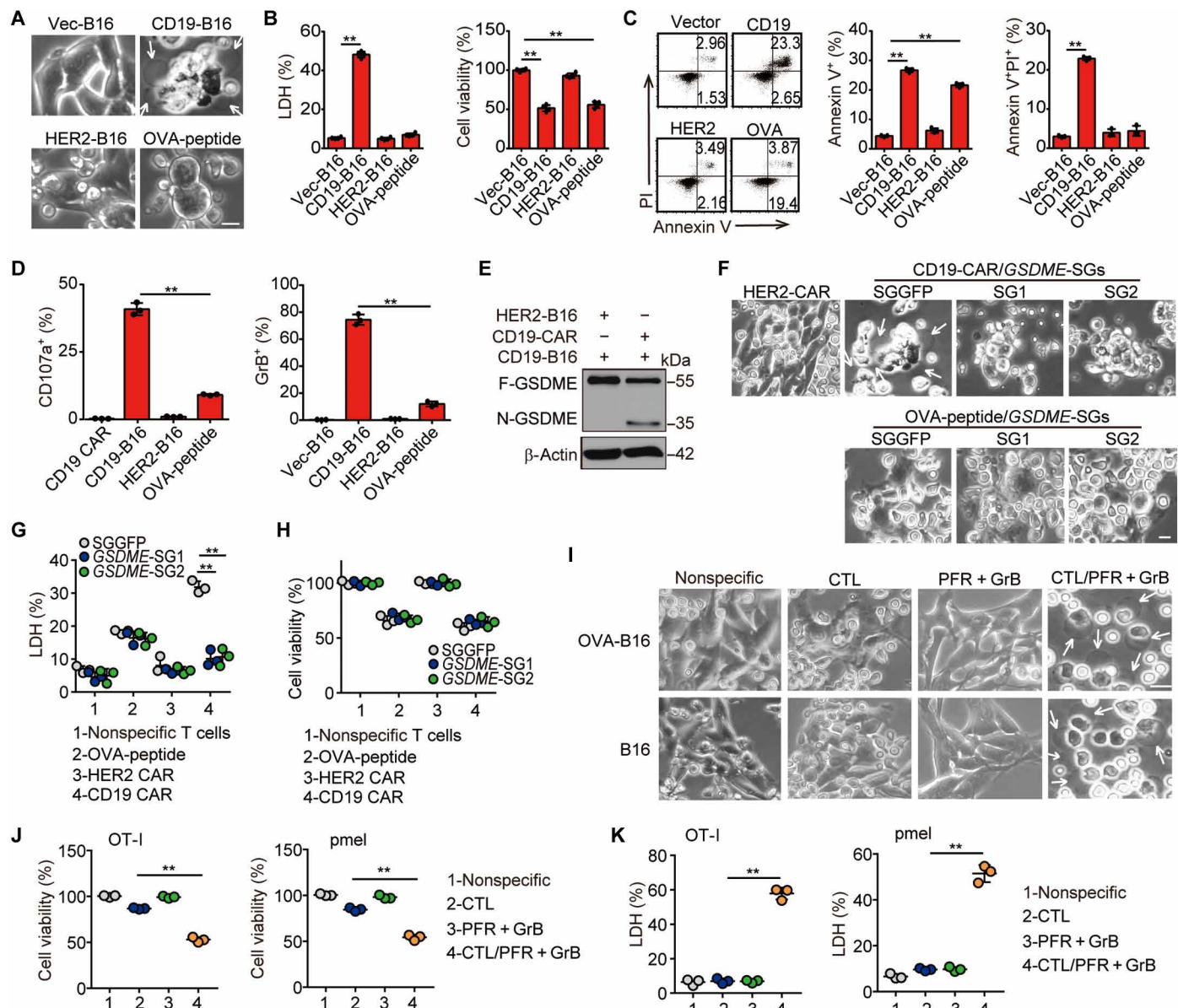


Fig. 4. Superior affinity is critical for CAR T cell-mediated tumor cell pyroptosis. (A to D) hCD19-mCAR T cells were cocultured with CD19-B16 (E/T = 2:1), HER2-B16 (E/T = 2:1), or vector-B16 pulsed with OVA peptide (E/T = 20:1) for 6 hours. Representative cell morphology was shown (A). LDH levels in supernatants, cell viability (B), and the annexin V⁺ or annexin V⁺/PI⁺ cells (C) were measured. The CD107a⁺ or GrB⁺ cells were determined by flow cytometry (D). White arrows indicate pyroptotic cells. (E) CD19-recognizing CAR OT-I T cells were cocultured with CD19 or HER2-B16 cells for 6 hours at a 2:1 E/T ratio. The expression of GSDME was determined by Western blot. (F to H) The same as (A), except that SGGFP or GSDME-SGs⁻ CD19-B16 cells were used. Cell morphology was observed by microscopy (F). The LDH level from the supernatant (G) was measured, and cell viability (H) was detected by a microplate luminometer. Scale bar, 20 μ m. (I) Luc-OVA-B16 or B16 cells were cocultured with tumor-specific CD8⁺ T cells in the presence or absence of 10 nM perforin and granzyme B. A representative image of cell death is shown (I). Six hours later, cell viability (J) and LDH levels (K) were measured. White arrows indicate the pyroptotic cells. **P < 0.01, by one-way ANOVA (B to D, G, J, and K). Data are means \pm SD of three independent experiments.

proinflammatory factors. We found that pyroptosis supernatants rather than GSDME^{-/-} supernatants caused the cleavage and activation of GSDMD (Fig. 6D). In addition, supernatants from nontransduced tumor-specific CD8⁺ T cell that killed target tumor cells did not induce cleavage of GSDMD or caspase 1 (fig. S6E). In addition, knockout of either GSDMD or caspase 1 abolished the up-regulation of IL-1 β and IL-6 in macrophages caused by pyroptosis supernatants (Fig. 6E and fig. S6, F to H). NACHT, LRR, and PYD domains-containing

protein 3 (NLRP3) is an inflammasome form that cleaves caspase 1 in macrophages. We found that pyroptotic supernatants could not effectively induce caspase 1 cleavage and subsequent mature IL-1 β production in NLRP3^{-/-} macrophages (fig. S7, A and B). Various factors such as reactive oxygen species (ROS), ions, and adenosine 5'-triphosphate (ATP) are able to activate the NLRP3 inflammasome (30). CD19 or HER2⁺ CAR T cell treatment led to a 14- to 26-fold increase of ATP concentration in the pyroptotic supernatants (fig. S7C). However,

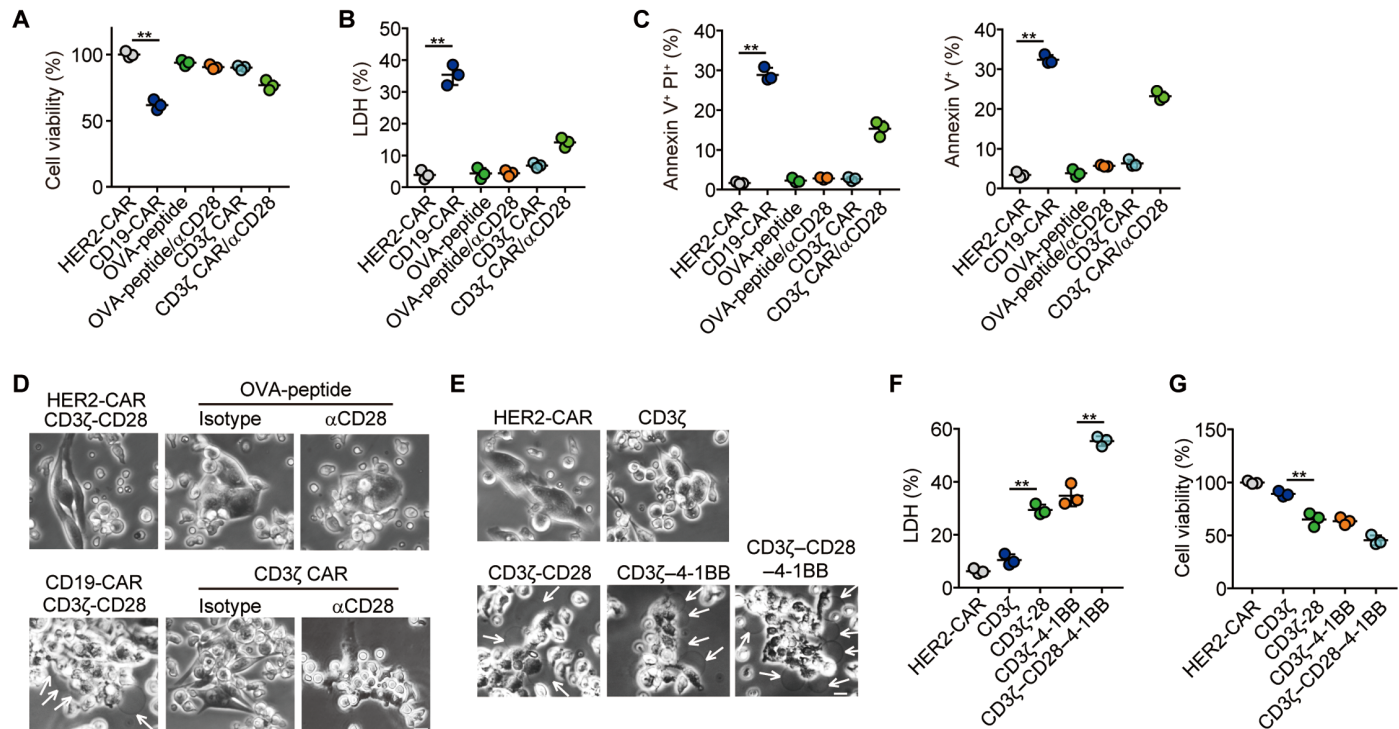


Fig. 5. Co-signaling domain(s) is important for pyroptosis by CAR T cells. (A to D) CD19-recognizing CD3ζ-CAR T cells were cocultured with CD19-expressing B16 cells in the presence of a CD28 antibody. Meanwhile, OT-I T cells were cocultured with OT-I peptide-pulsed, CD19-expressing B16 cells. CD3ζ-CD28-CAR T cells were used as a positive control. Cell viability was measured by a microplate luminometer (A), and the LDH level from the supernatant was detected (B). The percentage of annexin V⁺/PI⁺ or annexin V⁺ cells was determined by flow cytometry (C). Cell morphology was observed by microscopy (D). Scale bar, 20 μ m. (E to G) CD19-B16 cells were cocultured with HER2-CAR T cells or CD3ζ, CD3ζ-CD28, CD3ζ-4-1BB, or CD3ζ-CD28-4-1BB-CD19-CAR T cells for 4 hours. Cell morphology was observed under a microscope (E). The LDH level (F) and cell viability (G) were also measured. Scale bar, 20 μ m. **P < 0.01, by one-way ANOVA (A to C, F, and G). Data are means \pm SD of three independent experiments.

such an increase in ATP was abrogated by the inhibition of caspase 3 or granzyme B or by the knockdown of GSDME, perforin, or granzyme B (fig. S7, D to G). Apyrase is known to effectively degrade ATP (31), and treatment of pyroptotic supernatants with apyrase degraded ATP molecules in pyroptotic supernatants (fig. S7C), and this prevented pyroptotic supernatant-treated macrophages from cleaving caspase 1, GSDMD, or IL-1 β (fig. S7, H and I). A similar result was obtained in supernatants treated with Brilliant Blue G (BBG), an antagonist of the ATP-recognizing receptor P2X7 (fig. S7, H and I). Therefore, ATP from pyroptotic supernatants is sufficient to promote the release of the CRS-related cytokine IL-1 β by macrophages. Cell death can cause the release of DAMPs such as heat shock proteins (HSPs) and high-mobility group box 1 (HMGB1), and these can stimulate macrophages to produce IL-6 by activating mitogen-activated protein kinase (MAPK) and nuclear factor κ B (NF- κ B). We found much higher levels of HMGB1 in pyroptotic supernatants, compared with the non-pyroptotic supernatants, but levels of HSP70 were not altered (fig. S7J). Stimulation of macrophages with HMGB1 up-regulated the expression of IL-6 (fig. S7, K and L). In contrast, knockdown of HMGB1 in tumor cells disrupted the effect of the pyroptotic supernatant on IL-6 expression at both the mRNA and protein levels (fig. S7, M and N), suggesting that HMGB1 induces the IL-6 production in macrophages after tumor cell pyroptosis. Thus, HMGB1 in the pyroptotic supernatants may promote IL-6 expression in macrophages. Together, these results suggest that tumor cell pyroptosis activates the GSDMD-

mediated inflammatory pathway in macrophages, leading to the release of CRS-related cytokines.

CAR T cell therapy induces CRS through GSDME-mediated pyroptosis in vivo

Last, we tried to demonstrate that GSDME-mediated pyroptosis triggers CAR T cell therapy-caused CRS in vivo. We used a CAR T cell-induced CRS mouse model that used intraperitoneal injection of Raji or NALM-6 cells into severe combined immunodeficient (SCID)-beige mice, followed by an intraperitoneal injection of human CAR T cells, as described previously (8). An acute systemic inflammatory response, highly similar to human CRS, as depicted by high fever, weight loss, and increased levels of acute-phase proteins, such as serum amyloid A3 (SAA3), IL-1 β , and IL-6, was present (Fig. 7, A to E, and fig. S8, A to E). However, injection of GSDME^{-/-} Raji or NALM-6 cells in SCID-beige mice abrogated CRS symptoms upon CD19-CAR T cell treatment, as indicated by reduced weight loss, diminished fever, decreased blood levels of IL-1 β , IL-6, and SAA (Fig. 7, F to H, and fig. S8, F to H), and the prevention of CRS-related mortality (Fig. 7I and fig. S8I). We also examined intravenous injection of GSDME^{-/-} Raji cells into the non-obese diabetic SCID gamma (NSG) mice, and CRS symptoms and CRS-related mortality were also abrogated by GSDME deficiency (fig. S8, J to L), suggesting that GSDME-mediated pyroptosis may contribute to CRS during CAR T cell therapy. In line with these results, the knockout of GSDME in target tumor cells resulted

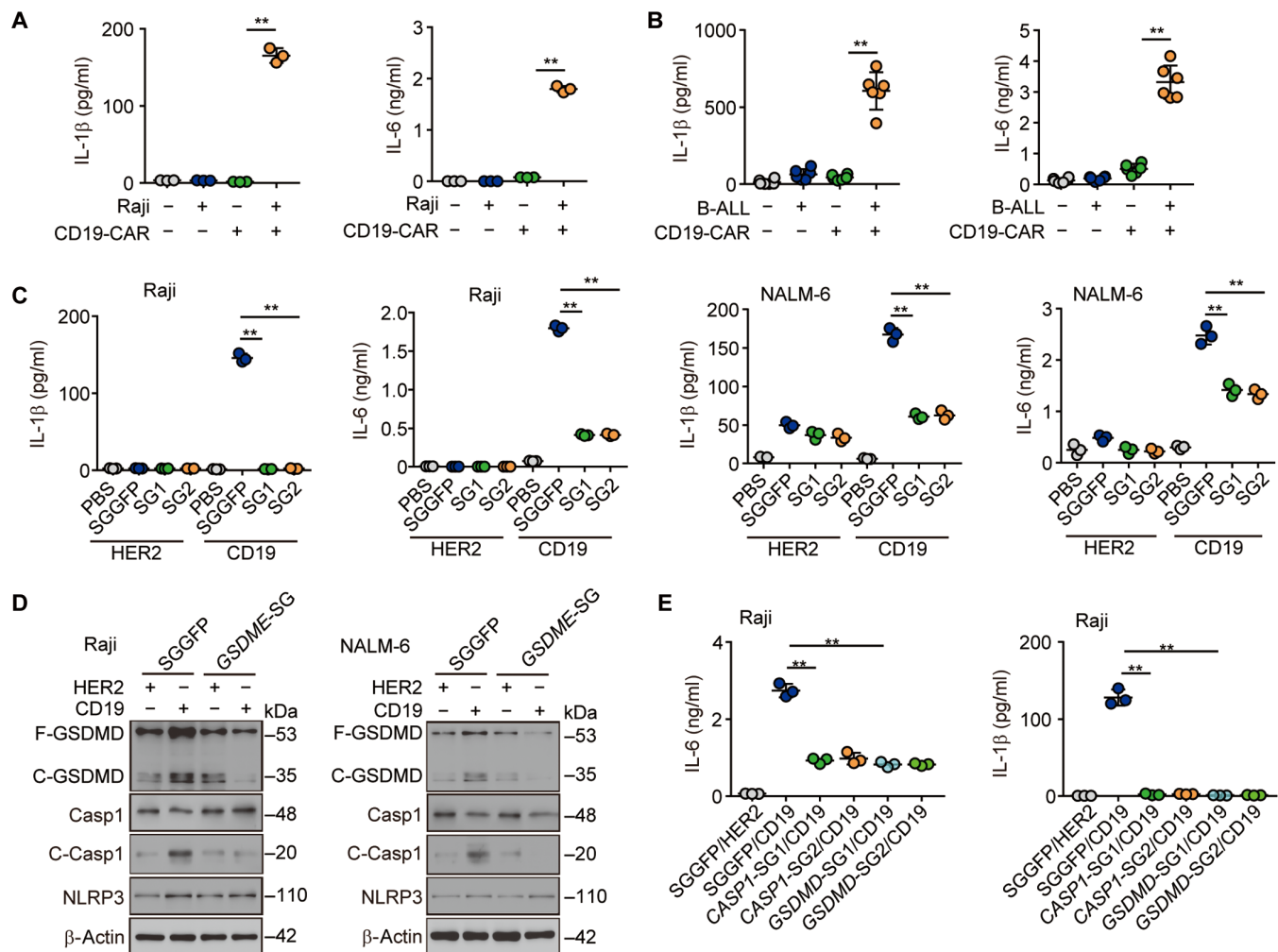


Fig. 6. Tumor cell pyroptosis triggered macrophages to release proinflammatory cytokines. (A) Macrophages isolated from healthy volunteers were treated with control or pyroptotic Raji supernatants. IL-1 β and IL-6 in the culture medium were determined by enzyme-linked immunosorbent assay (ELISA). (B) The same as (A), except that pyroptotic primary B leukemic cell supernatants were used. (C and D) Human macrophages were treated with supernatants from coculturing SGGFP or GSDME-SGs⁻ Raji or NALM-6 cells with or without CD19-CAR T cells. IL-1 β and IL-6 were determined by ELISA (C), and GSDMD, Casp1, C-Casp1, and NLRP3 were analyzed by Western blot (D). (E) SGGFP, CASP1-SGs, or GSDMD-SGs⁻ THP-1 cells were treated with supernatants from coculturing Raji cells and CAR T cells. IL-1 β and IL-6 were determined by ELISA. **P < 0.01, by one-way ANOVA (A to C and E). Data are means \pm SD of three independent experiments.

in a decreased serum ATP level in the CAR T cell-treated mice (fig. S8M). In addition, we found that the use of apyrase or BBG also abrogated the above CAR T cell therapy-induced CRS and prolonged survival (fig. S9, A to D), further suggesting that the CAR T cell–induced CRS is mediated through the GSDME-ATP pathway. The analysis of peritoneal macrophages confirmed the activation of caspase 1 and GSDMD (Fig. 7J) and the up-regulation of IL-1 β , IL-6, and SAA (Fig. 7, C to E) in the CAR T cell–treated mice. In contrast, the depletion of macrophages or the administration of a caspase 1 inhibitor prevented CAR T cell-associated CRS, as evidenced by decreased levels of SAA, IL-6, and IL-1 β ; reduced weight loss; diminished fever; and prolonged survival (Fig. 7, K to M). However, this prevention of CRS could be abolished by the intraperitoneal injection of exogenous wild-type (WT) macrophages but not *Gsdmd*^{-/-} or *Casp1*^{-/-} macrophages (fig. S9, E to H). To further validate these results in patients, we analyzed the GSDME levels in primary B-ALL leukemia cells isolated

from 11 patients before CD19-CAR T cell treatment. Although B leukemic cells from patients ubiquitously expressed GSDME (Fig. 7N), a higher level of GSDME was associated with a more severe case of CRS in those patients (Fig. 7O). ATP levels were found to be much higher in CRS patients than in healthy volunteers (fig. S9I). Moreover, patients with a high grade of CRS ($n = 7$) had higher blood LDH levels, compared with those with low grade of CRS ($n = 4$) (fig. S9J), and LDH levels positively correlated to the severity of CRS (Fig. 7P). Together, these results suggest that B leukemic cell pyroptosis induced by CAR T cell therapy triggers CRS in patients.

DISCUSSION

Genetic modification confers CAR T cells an enhanced ability to kill target tumor cells. The effects of the resulting massive tumor cell death on patients remain unclear. In this study, we show that CAR

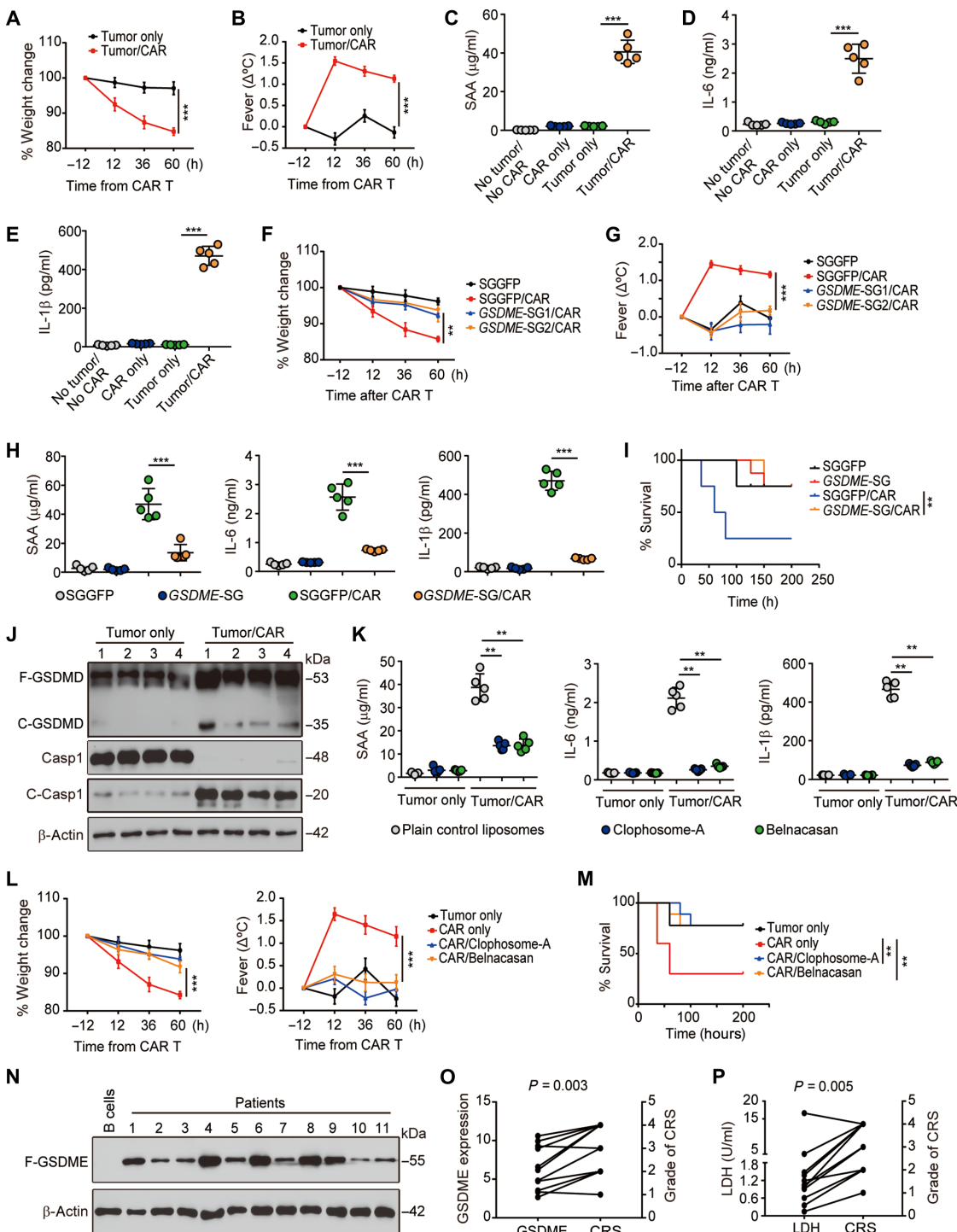


Fig. 7. Tumor cell pyroptosis triggers CRS in CAR T cell-treated mice. (A to E) CD19-CAR T cells were transferred to SCID-beige mice with a high Raji tumor burden. The change of weight [(A), $n = 6$] and body temperature [(B), $n = 6$] was calculated. The serum levels of SAA (C), IL-6 (D), and IL-1 β (E) were measured by ELISA ($n = 5$). (F to I) SGGFP⁺ or GSDME-SGs-Luc-Raji cells were intraperitoneally injected into mice for 3 weeks, followed by the intravenous injection of CD19-CAR T cells. Weight [(F), $n = 6$] and temperature [(G), $n = 6$] changes were calculated. Serum levels of SAA, IL-6, and IL-1 β were measured by ELISA [(H), $n = 5$]. Mice survival was analyzed [(I), $n = 10$]. (J) The same as (A), except that intraperitoneal macrophages were isolated to perform Western blot with anti-GSDMD, Casp1, and C-Casp1 ($n = 4$). (K to M) Mice with high Raji tumor burden were treated with a control liposome, clophosome-A (intravenous, 200 μl), or belnacasan (100 mg/kg) once daily for 3 days, followed by CD19-CAR T cell injection. Thirty-six hours later, serum levels of SAA, IL-6, and IL-1 β were measured by ELISA [(L), $n = 5$]. Weight and temperature changes were calculated [(L), $n = 6$]. Mouse survival was recorded [(M), $n = 10$]. (N) Primary B leukemic cells isolated from B-ALL patients ($n = 11$) were lysed for Western blot against GSDME. (O) Correlation between GSDME expression and grade of CRS ($n = 11$). (P) Correlation between LDH level and CRS grade ($n = 11$). ** $P < 0.01$, *** $P < 0.001$, by Student's t test (A and B), one-way ANOVA (C to H, K, and L) or by log-rank survival analysis (I and M). Data are means \pm SD.

T cells, by virtue of their release of a large amount of perforin and granzyme B, activate the caspase 3–GSDME pathway in B leukemic cells, leading to cell pyroptosis and subsequent CRS. CAR T cells have been observed to undergo an expansion process and reach an extremely high frequency at a certain time point *in vivo*. Thus, within a relatively short time, most targeted cells could undergo pyroptosis, causing stimulated macrophages to produce IL-6 and IL-1 β via activated caspase 1 and thus triggering CRS. The elucidation of this molecular mechanism provides an insight into the clinical observation that CRS severity is associated with the CAR T cell number and B leukemic cell burden during the CAR T cell therapy (5, 10–12).

The detection of GSDME expression in human B leukemic, MCF-7 breast cancer, and murine B16 melanoma cells is unexpected because it functions as a pore-forming protein, and its activation is potentially dangerous and may result in cell death. It has been reported that GSDME is not expressed in many detected tumor cell lines (17). In line with this, the promoter region of the *GSDME* gene displays a hypermethylation state (32, 33), thus indicating that the *GSDME* gene is silenced epigenetically in cells. GSDME is considered a tumor suppressor gene capable of inducing programmed cell death as a result of caspase 3 cleavage, and tumor cells may have evolved epigenetic means to silence GSDME expression to allow tumorigenesis. However, the high expression of GSDME in B leukemic cells and other tumor cells hints that GSDME probably exerts an alternative function to pore formation in tumor cells. The manner by which GSDME expression overcomes hypermethylation regulation and whether GSDME has a conventional function apart from pore formation are currently being investigated.

An important finding in this study is that CAR T cells release more perforin/granzyme B than nontransduced natural T cells. The release of cytolytic effector molecules by T cells relies on activation by two signals, MHC-antigenic peptide-TCR (signal 1) and CD80/CD86-CD28 (signal 2). Full activation of signal 2 relies on the activation strength of the TCR signaling. TCR signaling-activated LCK (light chain kinase) phosphorylates CD28 tyrosine residues; meanwhile, TCR signaling-activated LAT (linker of activated T cells) and SLP-76 phosphorylate and activate the key CD28 downstream signal molecule PLC- γ (phospholipase C- γ), thus degrading PIP₂ (phosphatidylinositol 4,5-bisphosphate) into DAG (diacylglycerol) and IP₃ (inositol 1,4,5-trisphosphate). On the basis of the understanding of T cell activation and the advances in genetic engineering, synthetic CARs are designed for human T cells. The basic concept for designing a CAR is to link a single-chain variable fragment (scFv) to CD3 ζ intracellular signaling module to induce T cell activation upon antigen binding. Currently, this modular structure has been extended from a single CD3 ζ signaling domain to the CD3 ζ -CD28, CD3 ζ -4-1BB, or CD3 ζ -CD28-4-1BB signaling domains to mimic both signal 1 and signal 2 (3). Because the affinity of CAR and its antigen may be 100-fold higher than that of the TCR and MHC-peptide complex (27, 28), this superior affinity plus the costimulatory signal confers CAR T cells the ability to release a large amount of perforin/granzyme B, which is required for CAR T cell-mediated target cell pyroptosis. Upon entering the cytoplasm, granzyme B may cleave pro-caspase 3 into its active form. Activated caspase 3 either induces apoptosis or cleaves GSDME to trigger pyroptosis through membrane pore formation. However, cells have the ability to rapidly heal pores in the plasma membrane. Whether GSDME triggers pyroptosis depends on the balance between membrane pore formation and membrane repair. Despite having the same amount of GSDME in target cells, natural TCR CD8 $^+$

T cells cause only low levels of cleaved GSDME, but CAR T cells release higher levels of perforin/granzyme B and result in a more activated GSDME.

Pyroptotic lysis is highly proinflammatory due to the release of cytosolic contents that are enriched in DAMPs. In this study, we demonstrate that tumor cell pyroptosis leads to the activation of caspase 1 and GSDMD in macrophages, leading to the release of a large amount of proinflammatory cytokines and the occurrence of CRS. Among proinflammatory cytokines, IL-6 and IL-1 β are especially important. Clinically, IL-6-neutralizing antibody is widely used to prevent and/or treat the CRS in CAR T cell-treated patients (34). As a pleiotropic cytokine, IL-6 is mainly regulated at the transcriptional level by transcription factors such as NF- κ B, AP-1 (activator protein 1), and STAT3 (signal transducer and activator of transcription 3) (35). Pathogen-associated molecular patterns (PAMPs), such as lipopolysaccharide (LPS), and DAMPs, such as HSPs and HMGB1, can stimulate macrophages to produce IL-6 through activation of these transcription factors (35, 36). We found that HMGB1 is present in pyroptotic supernatants, thus directly activating IL-6 in macrophages. IL-1 β is synthesized as a precursor form, and its release depends on activation of caspase 1, which is a proinflammatory caspase that is tightly regulated by inflammasomes. Inflammasome NLRP3 has been known to be widely activated by various stimuli, including microbial toxins, particulate matter, crystals, aggregated β -amyloid, or extracellular ATP (30). In this study, we found that pyroptotic supernatants contain ATP, and treatment with a P2X7 receptor antagonist or degradation of ATP inhibited the ability of pyroptotic supernatants to activate caspase 1 in macrophages. With the help of our mouse CRS model, we further demonstrated that the knockout of GSDME in target tumor cells, depleting macrophages or inhibiting caspase 1/GSDMD, can each block the occurrence of CRS. The elucidation of this molecular pathway is fundamental to better understand toxicity associated with CAR T cell therapy. A recent study by Staedtke *et al.* (37) showed that a catecholamine blocker can inhibit macrophages from releasing proinflammatory cytokines. Thus, a combined blockade of GSDME and catecholamine may result in a better treatment of CRS without diminishing tumor clearance.

Although this study reports that CAR T cells induce target tumor cell pyroptosis through a GSDME-dependent pathway, alternative pathway(s) might exist to mediate target cell pyroptosis by CAR T cells. Recent studies have reported that CAR T cells may mobilize TNF- α to mediate the killing process, which might be independent of granzyme B and perforin (38, 39). One possibility for this finding is that CAR T cells could use a two-step strategy to attack target cells. Granzyme B and perforin launch the first wave of killing, which could be followed by TNF- α if the target cells escape the first attack. This may also explain why pyroptosis can be blocked without considerably affecting CAR T cell-mediated killing. Our present study reveals the mechanistic difference between the type of cellular death caused by CAR and natural TCR T cells, which provides an opportunity to modify CAR to reduce CRS by switching target tumor cell death from pyroptosis to apoptosis.

Study design

The primary objective of the study was to elucidate the underlying mechanism of CRS occurrence. This study is a continuation of a previous investigation (40), in which we conducted a phase 1 clinical trial to evaluate the safety and efficacy of autologous CD19-CAR T cell treatment in patients with relapsed or refractory B-ALL (R/R ALL).

CD19-CAR T cells were generated ex vivo with the use of autologous T cells transduced with CD19 TCR- ζ /4-1BB lentiviral vector to express a CAR containing a CD3 ζ domain to provide a T cell activation signal and a 4-1BB domain to provide a costimulatory signal. Patients with R/R ALL were administered CD19-CAR T cells (1×10^6 to $1 \times 10^7/\text{kg}$) intravenously on days 0, 1, and 2 in the absence of disease progression or unacceptable toxicity. The clinical study protocol (ClinicalTrials.gov number NCT03156101) was approved by the First Affiliated Hospital of Zhengzhou University Institutional Review Board. The clinical investigation was conducted by the investigators in the First Affiliated Hospital of Zhengzhou University, and data were collected and analyzed at Institute of Basic Medical Science of Chinese Academy of Medical Sciences. All participants provided written informed consent before being enrolled in this study. For the in vitro study, CAR T or unmodified T cells were used to coculture with different tumor cells to determine tumor cell pyroptosis or apoptosis. We also used Cas9 technology to knock out different genes to elucidate how pyroptosis triggered CRS through a macrophage-dependent pathway in mouse models.

MATERIALS AND METHODS

Patients

To be eligible for participation in the study, patients had to be at least 4 years old at screening and no older than 70 years old and had been diagnosed as CD19 $^+$ relapsed or refractory B cell leukemia, who were not eligible for autologous or allogeneic stem cell transplantation and had limited prognosis (several months to <2-year survival) with currently available therapies; an Eastern Cooperative Oncology Group (ECOG) result of 0, 1, or 2; and stable vital signs. Other eligibility criteria were adequate heart, liver, and kidney function.

Human specimens

Human peripheral blood or bone marrow was obtained from patients at the First Affiliated Hospital of Zhengzhou University. Ethical permission was granted by the Clinical Trial Ethics Committee of the First Affiliated Hospital of Zhengzhou University. All patients provided written informed consent to participate in the study. The clinical features of the patients are listed in tables S1 to S5.

Animals and cell lines

Female SCID-beige or NSG mice, 6 to 8 weeks old, were purchased from the Center of Medical Experimental Animals of the Chinese Academy of Medical Science (Beijing, China). OT-I transgenic mice were gifted by H. Zhang (Sun Yat-sen University). Pmel-1 transgenic mice were presented by Y. Wan (Third Military Medical University). These animals were maintained in the Animal Facilities of Chinese Academy of Medical Science under pathogen-free conditions. THP-1 (acute monocytic leukemia cell line), SGC-7901 (gastric adenocarcinoma cell line), and MCF-7 (breast cancer cell line) and mouse tumor cell lines B16 and OVA-B16 (melanoma) were purchased from the China Center for Type Culture Collection (Beijing, China). Human tumor cell lines Raji (Burkitt's lymphoma cell line) and Nalm6 (acute lymphocytic leukemia cell line) were gifted by M. Wang (Chinese Academy of Medical Sciences and Peking Union Medical College). These cells were cultured in RPMI 1640 medium (Thermo Fisher Scientific) with 10% fetal bovine serum (FBS) (Gibco, USA), 2 mM L-glutamine (Gibco, USA), and 1% penicillin-streptomycin in a humidified atmosphere containing 5% CO₂ at 37°C.

Construction of human CD19 or HER2 $^-$ CAR T cells

The CAR for HER2 and CD19 was constructed as previously described (41, 42). In brief, the scFv fragment of HER2 from monoclonal antibody 4D5 or the scFv fragment of CD19 from clone FMC63 linked the CD8 α -chain hinge and transmembrane region with CD3 ζ and CD28 intracellular signaling domains, and this cassette was inserted into the lentiviral vector provided by the Obiooo Bioscience Company. The transduction procedure was initiated by stimulating CD8 $^+$ T cells with CD3/CD28 activator beads (Invitrogen) according to the instruction provided by the manufacturer with recombinant human IL-2 at a final concentration of 100 U/ml in X-VIVO 15 medium (Lonza) containing 5% FBS. Cells were harvested for lentiviral transduction on day 2 and resuspended in the same medium. The supernatants containing leviviruses were added to the medium at the multiplicity of infection of 1:10, and the plates were coated with RetroNectin [CH-296; Takara Bio, Otsu, Japan; coated using CH-296 (10 mg/ml)] according to the manufacturer. Then, cells were centrifuged at 1000g for 2 hours at 32°C and incubated at 37°C for 6 hours. The infection rates were quantified with flow cytometry after 2 days. In this study, the amount of CD19-CAR T cells was used according to the ratio of effector to target cells (2:1) or as indicated in the in vitro experiments. The T cells were transfected with lentivirus-CAR and cultured for 10 days for in vivo experiments. The transfection efficiency was evaluated by flow cytometry on days 3 and 5 after lentivirus transduction and at the end of culture. The transfection efficiency was around 40%. For in vitro experiments, we cultured CAR T cells for 5 to 7 days. These T cells grew logarithmically during the period of expansion. For clinical trial, we used CD3 ζ -4-1BB-CAR T. Otherwise, CD3 ζ -CD28-CAR T cells were used.

Construction of mCAR-hCD19

The sequences for mCAR-hCD19 contained the antigen receptor of human CD19 or HER2 scFv; the murine CD3 ζ , CD28, and/or 4-1BB; and the myc tag on the N terminus, as described before (43), and were synthesized by SyngenTech. This chimeric antigen construct was then cloned into a murine stem cell virus-green fluorescent protein (MSCV-GFP) (Clontech) murine retroviral vector (MSCV-myc-CAR-2A). Then, the Platinum-E (Plat-E) Retroviral Packaging Cell Line, Ecotropic cells (Cell Biolabs, RV-101) were transfected with mCAR-hCD19 plasmid and pCL-Eco retrovirus packaging plasmid to obtain retrovirus containing mCAR-hCD19. OT-I CD8 $^+$ T cells were activated with anti-CD3/CD28 beads (Gibco, 11453D), IL-2 (PerproTech, 212-12), and 55 μM β -mercaptoethanol (Gibco, 21985-023) for 24 hours. Then, OT-I CD8 $^+$ T cells were infected with the above virus in the presence of RetroNectin (Takara Bio) for 8 hours. Twenty-four hours later, the GFP-positive cells were sorted by flow cytometry using the BD Biosciences FACSaria II to obtain cells expressing high levels of hCD19 or hHER2.

CRS grades

The grading system of CRS is performed based on the clinical classification (44). In brief, grade 1 is that symptoms are not life threatening, such as fever, headache, myalgias, malaise, nausea, or fatigue; grade 2 includes symptoms that require and respond to intravenous fluids or low-dose vasopressors, grade 2 organ toxicity, or fraction of inspired oxygen less than 40%; grade 3 includes symptoms that require and respond to aggressive intervention (high-dose or multiple vasopressors), grade 3 organ toxicity or grade 4 transaminitis, or fraction of inspired oxygen equal or more than 40%; grade 4 can

manifest as life-threatening symptoms, grade 4 organ toxicity (excluding grade 4 transaminitis), or needing ventilator support; grade 5 is death. Grading of organ toxicities is performed based on CTCAE (Common Terminology Criteria for Adverse Events) v4.03 (45).

Quantification and statistical analysis

All experiments were performed at least three times. Results are expressed as means \pm SEM or means \pm SD, as indicated, and analyzed by two-tailed unpaired Student's *t* test or one-way analysis of variance (ANOVA), followed by Bonferroni's test. $P < 0.05$ was considered statistically significant. The analysis was conducted using the GraphPad 6.0 software. To analyze the correlation between the level of GSDME or LDH and the degradation of CRS, Pearson's correlation test was applied. The survival rates were performed by the log-rank test.

SUPPLEMENTARY MATERIALS

immunology.sciencemag.org/cgi/content/full/5/43/eaax7969/DC1

Materials and Methods

Fig. S1. CAR T cells induced tumor cells to enter pyroptosis.

Fig. S2. GSDME-mediated CAR T cell induced tumor cell pyroptosis.

Fig. S3. Perforin/granzyme B–caspase 3–GSDME pathway–mediated CAR T cell induced tumor cell pyroptosis.

Fig. S4. Tumor-specific CD8⁺ T cells induced tumor cells to enter apoptosis, not pyroptosis.

Fig. S5. High levels of perforin and granzyme B induce tumor cell pyroptosis.

Fig. S6. Tumor cell pyroptosis activated macrophages to release inflammatory cytokines.

Fig. S7. Pyroptotic tumor cells released ATP to activate macrophages.

Fig. S8. Tumor cell pyroptosis initiated CRS induced by CAR T cell therapy *in vivo*.

Fig. S9. ATP-Casp1-GSDMD pathway regulated the CRS induced by CAR T cell therapy *in vivo*.

Table S1. The general information from patients enrolled.

Table S2. Body temperature (°C) from B-ALL patients after CD19 CAR T cell therapy.

Table S3. Serum level of IL-6 (pg/ml) from patients after CAR T cell therapy.

Table S4. Serum level of IFN-γ (pg/ml) from patients after CAR T cell therapy.

Table S5. Serum level of IL-10 (pg/ml) from patients after CAR T cell therapy.

Movie S1. HER2⁺ m-Cherry–MCF-7 cells were cocultured with HER2-CAR T cells.

Movie S2. HER2⁺ m-Cherry–SGC-7901 cells were cocultured with HER2-CAR T cells.

[View/request a protocol for this paper from Bio-protocol.](#)

REFERENCES AND NOTES

1. S. S. Neelapu, F. L. Locke, N. L. Bartlett, L. J. Lekakis, D. B. Miklos, C. A. Jacobson, I. Braunschweig, O. O. Oluwole, T. Siddiqi, Y. Lin, J. M. Timmerman, P. J. Stiff, J. W. Friedberg, I. W. Flinn, A. Goy, B. T. Hill, M. R. Smith, A. Deol, U. Farooq, P. McSweeney, J. Munoz, I. Avivi, J. E. Castro, J. R. Westin, J. C. Chavez, A. Ghobadi, K. V. Komanduri, R. Levy, E. D. Jacobsen, T. E. Witzig, P. Reagan, A. Bot, J. Rossi, L. Navale, Y. Jiang, J. Aycock, M. Elias, D. Chang, J. Wiezorek, W. Y. Go, Axicabtagene ciloleucel CAR T-cell therapy in refractory large B-cell lymphoma. *N. Engl. J. Med.* **377**, 2531–2544 (2017).
2. S. L. Maude, T. W. Laetsch, J. Buechner, S. Rives, M. Boyer, H. Bittencourt, P. Bader, M. R. Verneris, H. E. Stefanski, G. D. Myers, M. Qayed, B. De Moerloose, H. Hiramatsu, K. Schlis, K. L. Davis, P. L. Martin, E. R. Nemecek, G. A. Yanik, C. Peters, A. Baruchel, N. Boissel, F. Mechinaud, A. Balduzzi, J. Krueger, C. H. June, B. L. Levine, P. Wood, T. Taran, M. Leung, K. T. Mueller, Y. Zhang, K. Sen, D. Lebwohl, M. A. Pulsipher, S. A. Grupp, Tisagenlecleucel in children and young adults with B-cell lymphoblastic leukemia. *N. Engl. J. Med.* **378**, 439–448 (2018).
3. M. Sadelain, I. Rivière, S. Riddell, Therapeutic T cell engineering. *Nature* **545**, 423–431 (2017).
4. C. L. Bonifant, H. J. Jackson, R. J. Brentjens, K. J. Curran, Toxicity and management in CAR T-cell therapy. *Mol. Ther. Oncolytics* **3**, 16011 (2016).
5. M. L. Davila, I. Rivière, X. Wang, S. Bartido, J. Park, K. Curran, S. S. Chung, J. Stefanski, O. Borquez-Ojeda, M. Olszewska, J. Qu, T. Wasieleswka, Q. He, M. Fink, H. Shinglot, M. Youssif, M. Satter, Y. Wang, J. Hosey, H. Quintanilla, E. Halton, Y. Bernal, D. C. Bouhassira, M. E. Arcila, M. Gonen, G. J. Roboz, P. Maslak, D. Douer, M. G. Frattini, S. Giralt, M. Sadelain, R. Brentjens, Efficacy and toxicity management of 19-28z CAR T cell therapy in B cell acute lymphoblastic leukemia. *Sci. Transl. Med.* **6**, 224ra225 (2014).
6. N. Frey, Cytokine release syndrome: Who is at risk and how to treat. *Best Pract. Res. Clin. Haematol.* **30**, 336–340 (2017).
7. D. T. Teachey, S. F. Lacey, P. A. Shaw, J. J. Melenhorst, S. L. Maude, N. Frey, E. Pequignot, V. E. Gonzalez, F. Chen, J. Finklestein, D. M. Barrett, S. L. Weiss, J. C. Fitzgerald, R. A. Berg, R. Aplenc, C. Callahan, S. R. Rheingold, Z. Zheng, S. Rose-John, J. C. White, F. Nazimuddin, G. Wertheim, B. L. Levine, C. H. June, D. L. Porter, S. A. Grupp, Identification of predictive biomarkers for cytokine release syndrome after chimeric antigen receptor T-cell therapy for acute lymphoblastic leukemia. *Cancer Discov.* **6**, 664–679 (2016).
8. T. Giavridis, S. J. C. van der Stegen, J. Eyquem, M. Hamieh, A. Piersigilli, M. Sadelain, CAR T cell-induced cytokine release syndrome is mediated by macrophages and abated by IL-1 blockade. *Nat. Med.* **24**, 731–738 (2018).
9. M. Norelli, B. Camisa, G. Barbiera, L. Falcone, A. Purevdorj, M. Genua, F. Sanvito, M. Ponzoni, C. Doglioni, P. Cristofori, C. Traversari, C. Bordignon, F. Ciceri, R. Ostuni, C. Bonini, M. Casucci, A. Bondanza, Monocyte-derived IL-1 and IL-6 are differentially required for cytokine-release syndrome and neurotoxicity due to CAR T cells. *Nat. Med.* **24**, 739–748 (2018).
10. S. L. Maude, N. Frey, P. A. Shaw, R. Aplenc, D. M. Barrett, N. J. Bunin, A. Chew, V. E. Gonzalez, Z. Zheng, S. F. Lacey, Y. D. Mahnke, J. J. Melenhorst, S. R. Rheingold, A. Shen, D. T. Teachey, B. L. Levine, C. H. June, D. L. Porter, S. A. Grupp, Chimeric antigen receptor T cells for sustained remissions in leukemia. *N. Engl. J. Med.* **371**, 1507–1517 (2014).
11. D. W. Lee, J. N. Kochenderfer, M. Stettler-Stevenson, Y. K. Cui, C. Delbrook, S. A. Feldman, T. J. Fry, R. Orentas, M. Sabatino, N. N. Shah, S. M. Steinberg, D. Stroncek, N. Tschernia, C. Yuan, H. Zhang, L. Zhang, S. A. Rosenberg, A. S. Wayne, C. L. Mackall, T cells expressing CD19 chimeric antigen receptors for acute lymphoblastic leukaemia in children and young adults: A phase 1 dose-escalation trial. *Lancet* **385**, 517–528 (2015).
12. J. H. Park, I. Rivière, M. Gonen, X. Wang, B. Senechal, K. J. Curran, C. Sauter, Y. Wang, B. Santomasso, E. Mead, M. Roshal, P. Maslak, M. Davila, R. J. Brentjens, M. Sadelain, Long-term follow-up of CD19 CAR therapy in acute lymphoblastic leukemia. *N. Engl. J. Med.* **378**, 449–459 (2018).
13. J. Shi, W. Gao, F. Shao, Pyroptosis: Gasdermin-mediated programmed necrotic cell death. *Trends Biochem. Sci.* **42**, 245–254 (2017).
14. D. Wallach, T.-B. Kang, C. P. Dillon, D. R. Green, Programmed necrosis in inflammation: Toward identification of the effector molecules. *Science* **352**, aaf2154 (2016).
15. J. Lin, S. Kumari, C. Kim, T.-M. Van, L. Wachsmuth, A. Polykratis, M. Pasparakis, RIPK1 counteracts ZBP1-mediated necroptosis to inhibit inflammation. *Nature* **540**, 124–128 (2016).
16. J. Yuan, P. Amin, D. Ofengheim, Necroptosis and RIPK1-mediated neuroinflammation in CNS diseases. *Nat. Rev. Neurosci.* **20**, 19–33 (2019).
17. Y. Wang, W. Gao, X. Shi, J. Ding, W. Liu, H. He, K. Wang, F. Shao, Chemotherapy drugs induce pyroptosis through caspase-3 cleavage of a gasdermin. *Nature* **547**, 99–103 (2017).
18. S. Rühl, K. Shkarina, B. Demarco, R. Heilig, J. C. Santos, P. Broz, ESCRT-dependent membrane repair negatively regulates pyroptosis downstream of GSDMD activation. *Science* **362**, 956–960 (2018).
19. U. Ros, A. Peña-Blanco, K. Hänggi, U. Kunzendorf, S. Krautwald, W. W.-L. Wong, A. J. García-Sáez, Necroptosis execution is mediated by plasma membrane nanopores independent of calcium. *Cell Rep.* **19**, 175–187 (2017).
20. J. Ding, K. Wang, W. Liu, Y. She, Q. Sun, J. Shi, H. Sun, D.-C. Wang, F. Shao, Pore-forming activity and structural autoinhibition of the gasdermin family. *Nature* **535**, 111–116 (2016).
21. J. Shi, Y. Zhao, K. Wang, X. Shi, Y. Wang, H. Huang, Y. Zhuang, T. Cai, F. Wang, F. Shao, Cleavage of GSDMD by inflammatory caspases determines pyroptotic cell death. *Nature* **526**, 660–665 (2015).
22. Y. Liu, T. Zhang, Y. Zhou, J. Li, X. Liang, N. Zhou, J. Lv, J. Xie, F. Cheng, Y. Fang, Y. Gao, N. Wang, B. Huang, Visualization of perforin/gasdermin/complement-formed pores in real cell membranes using atomic force microscopy. *Cell. Mol. Immunol.* **16**, 611–620 (2019).
23. X. Yang, H. R. Stennicke, B. Wang, D. R. Green, R. U. Janicke, A. Srinivasan, P. Seth, G. S. Salvesen, C. J. Froehlic, Granzyme B mimics apical caspases. Description of a unified pathway for trans-activation of executioner caspase-3 and -7. *J. Biol. Chem.* **273**, 34278–34283 (1998).
24. S. S. Metkar, B. Wang, M. L. Ebbs, J. H. Kim, Y. J. Lee, S. M. Raja, C. J. Froehlic, Granzyme B activates pro-caspase-3 which signals a mitochondrial amplification loop for maximal apoptosis. *J. Cell Biol.* **160**, 875–885 (2003).
25. I. Voskoboinik, J. C. Whisstock, J. A. Trapani, Perforin and granzymes: Function, dysfunction and human pathology. *Nat. Rev. Immunol.* **15**, 388–400 (2015).
26. A. H. Greenberg, Activation of apoptosis pathways by granzyme B. *Cell Death Differ.* **3**, 269–274 (1996).
27. J. D. Stone, A. S. Chervin, D. M. Kranz, T-cell receptor binding affinities and kinetics: Impact on T-cell activity and specificity. *Immunology* **126**, 165–176 (2009).
28. M. Chmielewski, A. Hombach, C. Heuser, G. P. Adams, H. Abken, T cell activation by antibody-like immunoreceptors: Increase in affinity of the single-chain fragment domain above threshold does not increase T cell activation against antigen-positive target cells but decreases selectivity. *J. Immunol.* **173**, 7647–7653 (2004).
29. J. A. Lopez, O. Susanto, M. R. Jenkins, N. Lukyanova, V. R. Sutton, R. H. Law, A. Johnston, C. H. Bird, P. I. Bird, J. C. Whisstock, J. A. Trapani, H. R. Saibil, I. Voskoboinik, Perforin forms

- transient pores on the target cell plasma membrane to facilitate rapid access of granzymes during killer cell attack. *Blood* **121**, 2659–2668 (2013).
30. O. Gross, C. J. Thomas, G. Guarda, J. Tschopp, The inflammasome: An integrated view. *Immunol. Rev.* **243**, 136–151 (2011).
 31. F. Ghiringhelli, L. Apetoh, A. Tesniere, L. Aymeric, Y. Ma, C. Ortiz, K. Vermaelen, T. Panaretakis, G. Mignot, E. Ullrich, J.-L. Perfettini, F. Schlemmer, E. Tasdemir, M. Uhl, P. Génin, A. Civitas, B. Ryffel, J. Kanellopoulos, J. Tschopp, F. André, R. Lidereau, N. M. McLaughlin, N. M. Haynes, M. J. Smyth, G. Kroemer, L. Zitvogel, Activation of the NLRP3 inflammasome in dendritic cells induces IL-1 β -dependent adaptive immunity against tumors. *Nat. Med.* **15**, 1170–1178 (2009).
 32. M. S. Kim, X. Chang, K. Yamashita, J. K. Nagpal, J. H. Baek, G. Wu, B. Trink, E. A. Ratovitski, M. Mori, D. Sidransky, Aberrant promoter methylation and tumor suppressive activity of the DNFA5 gene in colorectal carcinoma. *Oncogene* **27**, 3624–3634 (2008).
 33. K. Akino, M. Toyota, H. Suzuki, T. Imai, R. Maruyama, M. Kusano, N. Nishikawa, Y. Watanabe, Y. Sasaki, T. Abe, E. Yamamoto, I. Tarasawa, T. Sonoda, M. Mori, K. Imai, Y. Shinomura, T. Tokino, Identification of DNFA5 as a target of epigenetic inactivation in gastric cancer. *Cancer Sci.* **98**, 88–95 (2007).
 34. C. H. June, M. Sadelain, Chimeric antigen receptor therapy. *N. Engl. J. Med.* **379**, 64–73 (2018).
 35. S. Kang, T. Tanaka, M. Narazaki, T. Kishimoto, Targeting interleukin-6 signaling in clinic. *Immunity* **50**, 1007–1023 (2019).
 36. U. Andersson, H. Wang, K. Palmblad, A. C. Aveberger, O. Bloom, H. Erlandsson-Harris, A. Janson, R. Kokkola, M. Zhang, H. Yang, K. J. Tracey, High mobility group 1 protein (HMG-1) stimulates proinflammatory cytokine synthesis in human monocytes. *J. Exp. Med.* **192**, 565–570 (2000).
 37. V. Staedtke, R.-Y. Bai, K. Kim, M. Darvas, M. L. Davila, G. J. Riggins, P. B. Rothman, N. Papadopoulos, K. W. Kinzler, B. Vogelstein, S. Zhou, Disruption of a self-amplifying catecholamine loop reduces cytokine release syndrome. *Nature* **564**, 273–277 (2018).
 38. J. Michie, P. A. Beavis, A. J. Freeman, S. J. Vervoort, K. M. Ramsbottom, V. Narasimhan, E. J. Lelliott, N. Lalaoui, R. G. Ramsay, R. W. Johnstone, J. Silke, P. K. Darcy, I. Voskoboinik, C. J. Kearney, J. Oliaro, Antagonism of IAPs enhances CAR T-cell efficacy. *Cancer Immunol. Res.* **7**, 183–192 (2019).
 39. C. J. Kearney, S. J. Vervoort, S. J. Hogg, K. M. Ramsbottom, A. J. Freeman, N. Lalaoui, L. Pijpers, J. Michie, K. K. Brown, D. A. Knight, V. Sutton, P. A. Beavis, I. Voskoboinik, P. K. Darcy, J. Silke, J. A. Trapani, R. W. Johnstone, J. Oliaro, Tumor immune evasion arises through loss of TNF sensitivity. *Sci. Immunol.* **3**, eaar3451 (2018).
 40. Y. Liu, X. Chen, D. Wang, H. Li, J. Huang, Z. Zhang, Y. Qiao, H. Zhang, Y. Zeng, C. Tang, S. Yang, X. Wan, Y. H. Chen, Y. Zhang, Hemofiltration successfully eliminates severe cytokine release syndrome following CD19 CAR-T-cell therapy. *J. Immunother.* **41**, 406–410 (2018).
 41. R. A. Morgan, J. C. Yang, M. Kitano, M. E. Dudley, C. M. Laurencot, S. A. Rosenberg, Case report of a serious adverse event following the administration of T cells transduced with a chimeric antigen receptor recognizing ERBB2. *Mol. Ther.* **18**, 843–851 (2010).
 42. M. C. Milone, J. D. Fish, C. Carpenito, R. G. Carroll, G. K. Binder, D. Teachey, M. Samanta, M. Lakhral, B. Gloss, G. Danet-Desnoyers, D. Campana, J. L. Riley, S. A. Grupp, C. H. June, Chimeric receptors containing CD137 signal transduction domains mediate enhanced survival of T cells and increased antileukemic efficacy in vivo. *Mol. Ther.* **17**, 1453–1464 (2009).
 43. J. Chen, I. F. López-Moyado, H. Seo, C.-J. Lio, L. J. Hemptleman, T. Sekiya, A. Yoshimura, J. P. Scott-Browne, A. Rao, NR4A transcription factors limit CAR T cell function in solid tumours. *Nature* **567**, 530–534 (2019).
 44. S. S. Neelapu, S. Tummala, P. Kebraei, W. Wierda, C. Gutierrez, F. L. Locke, K. V. Komanduri, Y. Lin, N. Jain, N. Daver, J. Westin, A. M. Gulbis, M. E. Loghin, J. F. de Groot, S. Adkins, S. E. Davis, K. Rezvani, P. Hwu, E. J. Shpall, Chimeric antigen receptor T-cell therapy—Assessment and management of toxicities. *Nat. Rev. Clin. Oncol.* **15**, 47–62 (2017).
 45. U.S. Department of Health and Human Services, *Common Terminology Criteria for Adverse Events (CTCAE) Version 5.0* (U.S. Department of Health and Human Services, 2010).

Acknowledgments: We would like to thank all the participants and the staff at the First Affiliated Hospital of Zhengzhou University, Affiliated Cancer Hospital of Zhengzhou University, Peking University People's Hospital, and Union Hospital of Tongji Medical College for their support and aid during our study. **Funding:** This work was supported by the National Natural Science Foundation of China (81788101, 81661128007, 81530080, 81773062, 91942314) and Chinese Academy of Medical Sciences (CAMS) Initiative for Innovative Medicine (CAMS-I2M) 2017-I2M-1-001 and 2016-I2M-1-007. **Author contributions:** B.H. conceived the project. Y.L., Y.F., X.C., Z.W., T.Z., M.L., N.Z., J.L., K.T., J.X., Y.G., F.C., Y.Zhou, Z.Z., and Y.H. performed the experiments. B.H., Y.L., Y.F., X.C., X.Z., Q.G., and Y.Zhang developed methodology. B.H., Y.L., and Y.F. performed data analysis. Y.L. and Y.F. did the statistical analysis. B.H. and Y.L. wrote the manuscript. **Competing interests:** The authors declare that they have no competing financial interests. **Data and materials availability:** All data needed to evaluate the conclusions in the paper are present in the paper or the Supplementary Materials. Materials described in the study are either commercially available or on request from the corresponding author.

Submitted 23 April 2019
Resubmitted 28 August 2019
Accepted 19 December 2019
Published 17 January 2020
10.1126/sciimmunol.aax7969

Citation: Y. Liu, Y. Fang, X. Chen, Z. Wang, X. Liang, T. Zhang, M. Liu, N. Zhou, J. Lv, K. Tang, J. Xie, Y. Gao, F. Cheng, Y. Zhou, Z. Zhang, Y. Hu, X. Zhang, Q. Gao, Y. Zhang, B. Huang, Gasdermin E-mediated target cell pyroptosis by CAR T cells triggers cytokine release syndrome. *Sci. Immunol.* **5**, eaax7969 (2020).

Gasdermin E-mediated target cell pyroptosis by CAR T cells triggers cytokine release syndrome

Yuying Liu, Yiliang Fang, Xinfeng Chen, Zhenfeng Wang, Xiaoyu Liang, Tianzhen Zhang, Mengyu Liu, Nannan Zhou, Jiadi Lv, Ke Tang, Jing Xie, Yunfeng Gao, Feiran Cheng, Yabo Zhou, Zhen Zhang, Yu Hu, Xiaohui Zhang, Quanli Gao, Yi Zhang and Bo Huang

Sci. Immunol. **5**, eaax7969.
DOI: 10.1126/sciimmunol.aax7969

Gasdermin E as troublemaker

Cytokine release syndrome (CRS) is a complication associated with chimeric antigen receptor (CAR) T cell therapy in cancer patients. The mechanisms that trigger CRS are not clear, but Liu *et al.* describe a role for the pore-forming protein gasdermin E (GSDME) during tumor cell pyroptosis, which contributes to CRS. CAR T cells release granzyme B, which activates caspase 3 and cleaves GSDME in target tumor cells and causes pyroptosis. Pyroptosis by GSDME leads to activation of caspase 1 and GSDMD in macrophages, which is critical for triggering CRS. Elevated levels of GSDME in cancer patients positively correlated to CRS severity. In addition, the ability of CAR T cells to induce pyroptosis is associated with the levels of perforin and granzyme B released.

ARTICLE TOOLS

<http://immunology.science.org/content/5/43/eaax7969>

SUPPLEMENTARY MATERIALS

<http://immunology.science.org/content/suppl/2020/01/13/5.43.eaax7969.DC1>

REFERENCES

This article cites 44 articles, 10 of which you can access for free
<http://immunology.science.org/content/5/43/eaax7969#BIBL>

Use of this article is subject to the [Terms of Service](#)

Science Immunology (ISSN 2470-9468) is published by the American Association for the Advancement of Science, 1200 New York Avenue NW, Washington, DC 20005. The title *Science Immunology* is a registered trademark of AAAS.

Copyright © 2020 The Authors, some rights reserved; exclusive licensee American Association for the Advancement of Science. No claim to original U.S. Government Works